Nature Environment and Pollution Technology
An International Quarterly Scientific Journal

p-ISSN: 0972-6268
(Print copies up to 2016)
e-ISSN: 2395-3454

Vol. 24 | No. S1 | pp. 19-40 | 2025

Original Research Paper

https://doi.org/10.46488/NEPT.2025.v24iS1.002

Open Access Journal

Exploring the Nexus Between Urban Land Use/Land Cover (LULC) Changes and Urban Growth Analysis Using Geoinformatics in Tumkur City, India

A. Kishor Kumar, Govindaraju†, C. J. Rakesh and S. Lokanath
Department of Applied Geology, Kuvempu University, Shankaraghatta-577 451, Karnataka, India
†Corresponding author: Govindaraju; drgov@yahoo.com

Nat. Env. & Poll. Tech.
Website: www.neptjournal.com

Received: 29-02-2024
Revised: 20-05-2024
Accepted: 22-05-2024

Key Words:
Annual Urban Spatial Expansion Index
Urban Expansion Intensity Index
Annual Built-up Change Index
Land use/Land cover
Urban sprawl

ABSTRACT

For the past several decades, Tumkur has been one of the fastest-developing cities in Karnataka. Hence, an assessment concerning the identification of LULC mutations and their intensity and urban sprawl in Tumkur City has been employed using cutting-edge Geospatial techniques. In this study, multi-temporal satellite imagery such as Landsat 5 (2000), Resourcesat-1 (2005, 2009 & 2012), and Sentinel-2A (2015 & 2020) were utilized to monitor historical LULC changes, land transformation, direction of urban growth and sprawl. The outcome of the change detection demonstrates that between 2000 and 2020, the built-up area expanded significantly, from 24.94 km^2 to 60.59 km^2. Consequently, the land transformation matrix analysis shows that substantial modifications in LULC have occurred over the period, with a rise in built-up areas and plantations and a decline in agricultural land, water bodies, and scrubland. Further, urban expansion analysis using UEII (Urban Expansion Intensity Index) revealed that most of the area is in the fast-paced stage of urban expansion. Moreover, two well-known indices; the Annual Urban Spatial Expansion Index (AUSEI) and the Annual Built-up Change Index (ABCI), show a significant positive correlation between them (R^2 = 0.69) justifying the increased urban growth in the study area. Whereas, built-up density and the Annual Urban Spatial Expansion Index (AUSEI) show a negative correlation (R^2 = 0.55) indicating the presence of compactness of the core of the city. Apart from the above analysis, urban sprawl was effectively interpreted using zones formed using Shannon entropy; NNE, ESE, and SSW have high urban sprawl due to National Highways, growth of Industries, and infrastructure activities developed by the government. Further, the present study's findings will contribute to understanding land use dynamics, urban sprawl, urban growth analysis, and future projections, as well as provide crucial information for decision-making and urban planning processes, to the urban planner to support acceptable land use management and guiding plan for appropriate growth of urban areas.

INTRODUCTION

Globally, 3500 million people live in towns; by 2030, this number will rise to 6000 million (Bunyangha et al. 2021, Sustainable Development Goal 2021). As per the World Urbanization Prospects (2018) study In the future, 95% of the urban population will settle in developing countries. During this metamorphosis, the natural environment changes dramatically as human activities alter and adapt to enable urbanization (Brown et al. 2000, Montgomery et al. 2013). Several factors, including the progress of population explosion, economic progression, industrialization, and infrastructure blossoming, facilitate the expansion of urban areas (Marcotullio & Lee 2003, Dahly & Adair 2007, Rauws & de Roo 2011, Padhi & Mishra 2022). The above factors have often been described as the direct consequence of urban expansion; these factors directly lead to an increased need for land resources resulting in the alteration of land use and land cover in a specific region. In addition, urban areas exhibit distinctive characteristics that are unique to them from rural and natural environments (Lambin et al. 2001, Maktav & Erbek 2005, Yakub & Tiffin 2017, Yin et al. 2023, Burgalassi et al. 2015). The most crucial factor behind global ecosystem modifications is transforming indigenous land cover types into artificial land use types (Dutta et al. 2020, Antipova et al. 2022). As a result, the investigation of LULC trends can serve as a basis for managing and planning natural resources at various spatial and time scales (Turner et al. 1994, Khan & Jhariya 2018).

The rate of urbanization in India slowed at first but began rising steadily in the 1920s (Mohan & Dasgupta 2004, Dadras et al. 2015). Due to industrial evolution and the increase in population growth, most people's forces commute daily to the suburbs, resulting in LULC changes (Kasraian et al. 2017, Haque & Basa 2017). Infer that conversion of

agricultural and other natural land cover types into urban areas, the urban areas have begun to expand outward (Dutta et al. 2020, Antipova et al. 2022). As a result of the analysis of LULC alterations, a plausible explanation is given for the relationship between man and the environment in the past and coming years (Lu et al. 2019, Dijoo 2021). Thus, LULC studies have the potential to help solve pressing environmental problems such as urban heat islands, pollution, global warming, loss of biodiversity climate change, and disasters, etc (Mathews & Nghiem 2021, Mohamed & Worku 2019, Yan et al. 2019, Herold et al. 2003).

The changes in LULC directly impact the urban ecosystem which imposes the establishment of sustainable urban areas (Ning et al. 2022). Nevertheless, the objective of eco-friendly urban development is to establish cities and communities that are ecologically, financially, and socially viable (Grekousis et al. 2013, Liu et al. 2019). In addition, landscape ecology and metrics can also be used to describe spatiotemporal variations and dynamics associated with the enlargement of urban centers and changes in land use caused by human activities (Yang et al. 2003, Masila 2016). It has been shown that land use and land cover can be classified, and growth in urban areas can be analyzed using a variety of techniques like Remote Sensing (RS) and Geographical Information Systems (GIS) (Jaad & Abdelghany 2021). Various methods, including unsupervised and supervised classification (Kim 2016, Didier et al. 2012), applying different indices, principal component analysis (Deng et al. 2008, Ji et al. 2006), hybrid methods (Mas et al. 2017, Grodach et al. 2022), and object-based detection methods were utilized to quantify, assess, map, and monitor urban growth.

In the present study, we utilized the geospatial method to evaluate land use and land cover changes and urban growth analysis in the study area. Scholars have utilized a few important indices to monitor and analyze urban expansion in a given area. These are Shannon's entropy, Urban Expansion Intensity Index, Built-up Density, Annual Urban Spatial Expansion Index, and Annual Built-up Change Index.

An emerging urban entity in Karnataka named Tumkur City, located near Bangalore City, is experiencing significant progress and improvement of infrastructure. As a result of notable changes in some sectors, including administration, economy, culture, and education, the city has experienced significant transformations. Few research works were carried out on urban-related matters however, no single study was carried out on urban land transition using geospatial technology. Despite this, the study area has undergone prodigious development of the urban over the past few generations. In this context, our study seeks to fill this research gap by integrating the LULC dynamics of the study area using remote sensing and geographic information systems. The specific objectives of the study are as follows: (a) to scrutinize the spatiotemporal changes of LULC in the study area between 2000 and 2020, (b) to interrogate the sprawling rate of the Tumkur City area, and (c) to schematize the pattern of urban growth using three relevant indicators, such as the AUSEI, BUDI, and ABCI. Using these scientific conclusions of the study area's past and present land-cover scenarios, planners/decision-makers can devise sustainable urban development strategies, and ecological sustainability plans will remain vital for future generations.

STUDY AREA

In Karnataka, Tumkur is one of the foremost important industrial hubs. It lies between the latitudes 13°19'00 and 13°21'19" and the longitudes 77°05'26" and 77°07'12. The Indian government picked one of seven smart cities in Karnataka as part of the Smart City Mission. In 1961, the area of Tumkur City was 12.95 km^2, in 2011, it was 64.27 km^2 (Fig. 1). According to the master plan map for 2021, it was 331.6 km^2. It is roughly 65 kilometers from the capital of Karnataka, Bangalore. Because of its nearness to the capital, the scarcity of affordable land in Bangalore, and the accessibility of resources within the study area, it is a prime site for growth in industry. It is an ideal location for setting up industries along National highways (NH 48 and NH 73). As a result of the study area, several small, medium, and large industries have been established. Four industrial areas and seven industrial estates are located in the study region. In total, four industrial areas are located in Hirehalli, Satyamagala, Arthasanahalli Phase 1, and Arthasanahalli Phase 2. A rapidly expanding population (Table 1 and Fig. 2), new infrastructure development, and the opening of new advanced industries have substantially altered Tumkur City's land use and cover classes.

MATERIALS AND METHODS

Materials

Landsat 5, Resourcesat-1, and Sentinel-2A imagery were used to perform a LULC change study. The topographic maps of India were used in the research region and utilized as ground validation. ERDAS IMAGINE & Arc GIS software was used to create land use maps to fully understand the dynamics of urban growth patterns and examine LULC changes. LULC maps have been verified by Google Earth Pro samples as well as ground truth surveys. The satellite imagery employed for this research is presented in Table 2.

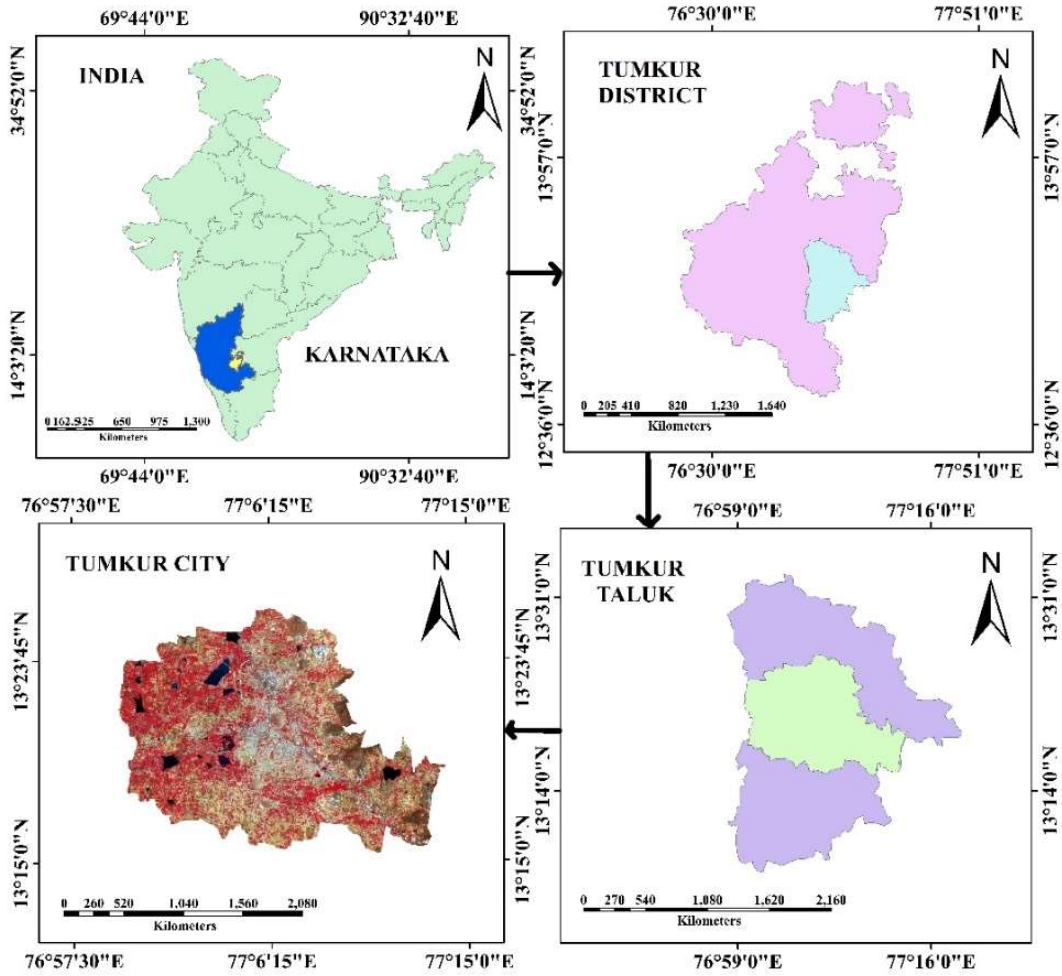

Fig. 1: The location map of the study area.

Table 1: Population-level and growth rate for the Tumkur, from 2000 to 2020.

Year	Population Data	Growth Rate
2020	361,000	1.69%
2019	355,000	2.01%
2018	348,000	1.75%
2017	342,000	2.09%
2016	335,000	1.82%
2015	329,000	2.17%
2014	322,000	1.90%
2013	316,000	1.94%
2012	310,000	1.97%
2011	302143	2.01%
2010	298,000	1.71%
2009	293,000	2.09%
2008	287,000	2.14%
2007	281,000	1.81%
2006	276,000	1.85%
2005	271,000	1.88%
2004	266,000	2.31%
2003	260,000	1.96%
2002	255,000	1.59%
2001	248929	2.87%
2000	244,000	3.39%

(Source: United Nations population projections and Census of India 2011)

Modeling Framework

The study uses remote sensing and geographic information systems to measure land use, land cover changes, and transformation matrics in Tumkur City during the last two decades. As a result, these metrics can shed insight into the extent and nature of land transformations and assist in

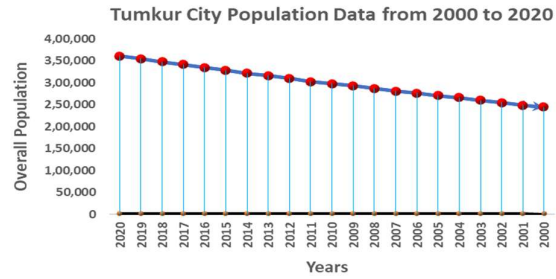

Fig. 2: Column graph of the population growth rate of Tumkur City (2000-2020).

Table 2: Various satellite images were incorporated into the study.

Sl No	Satellite Images	Resolution (in meters)	Path/Row	Observation Date	Source
1	Landsat 5	30	144/51	16/03/2000	USGS Earth Explorer
2	Resourcesat-1	23.5	93/56	06/08/2005	Bhuvan Geo Platform of ISRO
				31/03/2009	
				08/02/2012	
3	Sentinel – 2A	10	-	10/22/2015	Copernicus open-access hub
				02/03/2020	

understanding the dynamics of urban landscapes. As part of the study, five important indices are also used to measure specific aspects of urbanization. As part of the study, five important indices are also used to measure the impacts of town growth. The study area's Urban Area Expansion Intensity Index is used to determine the city's speed and rate of urbanization. In addition, the Shannon entropy measures the degree to which urban sprawl has been compacted or dispersed. A built-up density index can be used to estimate the urban area per unit of the total landscapes. The AUSEI (Annual Urban Spatial Expansion Index) measures the annual rate of urban growth in urban areas as well as the annual expansion of urban space (Dutta et al. 2019, Zhang et al. 2022). The Annual Built-Up Change Index (ABUCI) helps to provide some insight into the spatiotemporal variation in land conversion, a primary factor driving urban growth (Xie et al. 2005). BI, AUSEI, and ABUCI were intercorrelated analyses of urban growth in the form of a graph between 2000 and 2020.

Image Pre-Processing and Land Use Land Cover Analysis

Pre-processing satellite pictures facilitates recognizing atmospheric noise, such as haze created by water vapor, smog, and atmospheric components. It is necessary for obtaining meaningful and reliable findings in remote sensing. It offers a variety of methods for analyzing the standard results of images to determine the accuracy of surface features. Arc Map 10.4 and ERDAS Imagine Software (2014) was employed to find the atmospheric correction present in the satellite images and to generate apparent reflectance. Apart from that geometric correction, Edge enhancement, and Image Filtering techniques were done to analyze the error in rectification, coordinates problem, and altitudes error. These methods are useful to improve the quality of satellite images for classification. However, land use and land cover classification is essential for analyzing the information through satellite images and knowing the arrangement of different LULC classes within the study area. Using the supervised classification method like the Gaussian Maximum Likelihood Classifier Algorithm (GMLCA) used to create land use and land cover maps of satellite images from 2000, 2005, 2009, 2012, 2015 and 2020.

Based on the NRSC level III classification scheme, eleven land use and land cover classes were classified: Scrub Forest, Forest Plantation, Water Bodies, Built-up, Double Crop, Scrubland, Land without Scrub, Fallow Land, Stony Waste, Kharif Crop, and Plantations. The LULC maps have been verified on the ground using Google Earth Pro samples. Finally, multi-temporal rasters were prepared for 2000, 2005, 2009, 2012, 2015, and 2020, and their corresponding statistics were compared to determine the transition in landscape patterns.

Land Use/Land Cover Change Dynamic Index

LU/LC change Dynamic Index is also called as Land change Dynamic Index. It used to evaluate the degree of dynamism of each class, the dynamic LULC change index examines the provided LULC classes. The following formula (1) explains how to calculate the change dynamic index (Zhang Hong et al. 2011).

$$K = \sum \frac{1}{T} * \frac{U_b - U_a}{U_a} \times 100 \quad \ldots(1)$$

Where K is the LULC Change Dynamic Index, U_a is an area of a certain LULC type at the initial year, U_b is an area of a certain LULC type in the final year, and T is the length of time.

Accuracy Assessment

A LULC classification's accuracy and correctness are evaluated through accuracy assessment (Ma & Redmond 1995, Sun et al. 2020). As a result, it is possible to assess the quality and reliability of classified maps, ensuring that they meet their intended purpose. The Kappa coefficient was used to assess the accuracy of land use and land cover classification at 120 randomly selected sites throughout the research region. The analysis was conducted using Ground Control Points (GCP) obtained from Google Earth Pro and a field survey.

$$KC = \frac{\sum_{i=1}^{k} nii - \sum_{i=1}^{k} nii(GiCi)}{n2 - \sum_{i=1}^{k} nii(GiCi)} \quad \ldots(2)$$

Estimation of Land Transformation Matrix

Evaluating a land transformation matrix is a useful way to find out how land cover and usage have changed in a specified time (Munsi et al. 2010, Roy & Roy 2010, Kindu et al. 2013, Mishra & Rai 2016a,b, Younes et al. 2023). The matrix tabulation provides necessary information regarding how the area of land classes encroached on others and shows the gains and losses related to a particular class (Naikoo et al. 2020). For measuring the extent of land transformation, we created five maps (2000–2005, 2005–2009, 2009–2012, 2012–2015, and 2015–2020) and analyzed the attributes table in ArcGIS to determine the area of different land classes. Preparation of land transformation matrix based on Equation. 3:

$$A \cdot B \times C = A \times B \cdot C = \begin{pmatrix} S_{11} & S_{12} & \ldots. & S_{1n} \\ S_{11} & S_{22} & \ldots. & S_{2n} \\ \vdots & \vdots & & \\ S_{n1} & S_{n2} & \ldots & S_{nn} \end{pmatrix} S \sum_{j=1}^{N} Sij \quad \ldots(3)$$

Measuring Urban Area Expansion Intensity Index

The Urban Expansion Intensity Index, or UEII, is an effective tool for assessable estimation of urban spatial expansion variations (Yan et al. 2019). It calculates the level of urbanization and the rate at which urban landscapes are expanding or contracting (Zhong et al. 2020). It is an indicator that takes into account both the length of expansion and the proportional growth in the size of urban areas. To calculate the UAEII, the equation (4) has been used:

$$UAEII = \frac{UA^{t2}{}_b - UA^{t1}{}_b}{TA_b * \Delta t} \times 100 \quad \ldots(4)$$

[Where, UA = Urban area; b = spatial unit; t1 = initiatory year; t2 =finale year; Δt = t2 - t1; TA = Total landscapes of the appraisal field.

There are five categories in the UEII standard: leisurely - rapidity elaboration (0 to 0.28), low- rapidity elaboration (0.28 to 0.59), medium- rapidity development (0.59 to 1.05), high- rapidity development (1.05 to 1.92), and extremely high- rapidity elaboration >1.92. (Zhong et al. 2020).

Urban Sprawl Analysis Using Entropy Model

Shannon's entropy: The Shannon entropy index is the only method of evaluating urban sprawl that is widely used and widely accepted (Bhatta et al. 2010b). Shannon's entropy (Hn), is used to detect and approximately estimate urban sprawl (Bhatta et al. 2010).

Shannon's entropy is given by:

$$H_n = -\sum piloge(pi) \quad \ldots(5)$$

Where n is the total number of zones in the region, and Pi is the portion of the variable in the ith zone. In this study, eight subregions are identified (NNW, NNE, WNW, ENE, WSW, SSW, ESE, SSE) by vertical and horizontal grid lines that intersect at the city center (CBD), from which urbanization has spread along trunk corridor roads to the peripheral areas (Felix Ndidi Nkeki 2016). Shannon's entropy value ranges from 0 to loge (n), and values close to 0 and log (n) indicate a scattered distribution and compactness within urban areas. When entropy values (larger) close to loge (n) indicate a dispersion of urban areas or urban patches, urban sprawl is considered to be occurring (Felix Ndidi Nkeki 2016).

Graphical Analysis of Urban Growth Monitoring Using Indices

Built-up density index (BUDI): Built-up density is a major indicator for measuring the connection between the total built-up area and the total area of a geographical unit. Using this index, a region can determine its level of urbanization ratio has changed as a result of the rapid spread of the urban field, which has increased the density of the built-up area. In addition to indicating new construction locations, this index also indicates the pattern and course of urban expansion. The built-up density is calibrated using Equation 6 (Dutta et al. 2019).

$$BD = \frac{UA}{ZA} \quad \ldots(6)$$

BD is the built-up density, UA is the total Built-up area of the zone, and ZA is the total area of the zone.

Annual Urban Spatial Expansion Index (AUSEI): It is possible to calculate the amount of land transformed into built-up land using satellite data based on essential change detection. Tumkur City has developed a yearly urban spatial expansion index to measure the spatiotemporal changes in urban growth (Wang et al. 2023). It is employed for assessing the temporal change in urban regions. The annual Urban Spatial Expansion Index can be calculated using equation (7):

$$\text{AUSEI} = \frac{B_a - B_{ao}}{B_a(a - a_0)} \times 100 \quad \ldots(7)$$

where $Ba - Ba_0$ is the total town area in square kilometers at the time a (finale year) and time a_0 (initiatory year) (Dutta et al. 2019).

Annual Built-up Change Index (ABUCI): More impermeable surfaces have been created since rural areas have been converted to urban areas. The rapidity of land-use change must be quantified and to assess the conversion process relating to the development and growth of urban areas it is very essential. Expansion of urban areas occurs when the current land use and land cover are altered. Consequently, changes in built-up areas are linked to urban development. Observing spatiotemporal variation in the land conversion process, one of the primary motors of urban growth is possible by examining the annual change in built-up areas (Dutta et al. 2019). Annual Builtup Change Index calculated using equation (8).

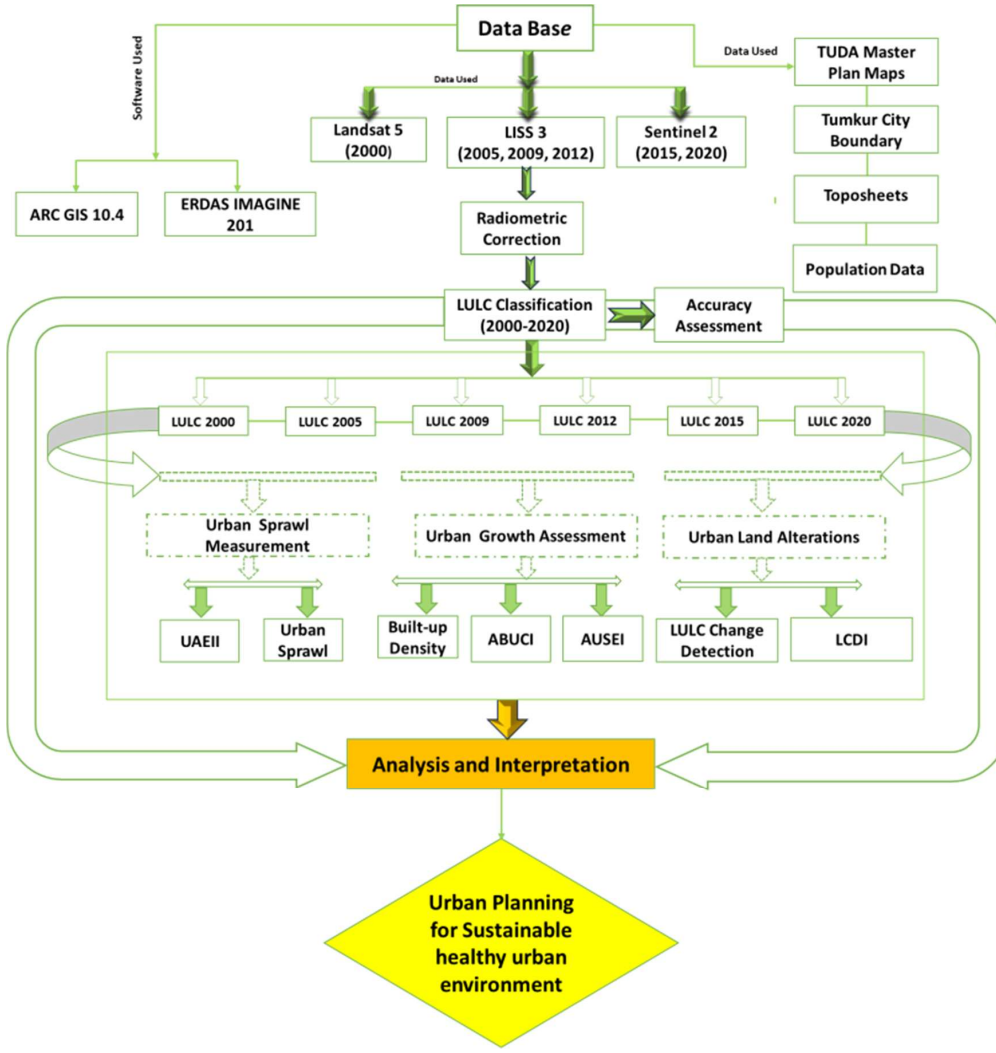

Fig. 3: Schematic representation of the methodology.

$$ABUCI = \frac{U_t - U_{to}}{t - t_0} \times 100 \quad \ldots(8)$$

where $U_t - U_{to}$ is the total urban area in square kilometers at time t (final year) and time t_o (initial year) (Dutta et al. 2019). Fig. 3 shows the schematic representation of the methodology.

RESULTS AND DISCUSSION

Spatio-Temporal Changes of Land Use and Land Cover Pattern

A maximum likelihood classifier was used to create a land use and land cover map of the study area for the years 2000 (Landsat), 2005, 2009, 2012, (Resourcesat-1), 2015 2020 (Sentinel-2) using various satellite images (Fig. 4). The accuracy assessment result shows that the overall accuracy values are 87%, 88%, 86%, 92%, and 94% in the years 2000, 2005, 2009, 2012, 2015 and 2020, respectively, and also corresponding kappa co-efficient are 0.80, 0.82, 0.84, 0.91, 0.92 and 0.94, respectively. The land use and land cover statistics from 2000 to 2020 are shown in Table 3.

Land use and land cover pattern of 2000: The most dominant land use in the study area is kharif, covering an area of 154.46 km^2, accounting for 48% of the study area. The Hemavati River has supplied water to lakes of the Tumkur City since 1990. The availability of water in tanks has led to a gain in the area of plantations in the study region. Tumkur has a high concentration of agricultural fields due to its diverse cropping patterns, fertile soil, irrigation infrastructure, and government policies that promote agriculture. The plantations and water bodies is land use covered the area of 61.57 km^2 and 24 km^2, respectively. Different types of LULC classes were observed, such as scrub land covering 11.30 km^2, built-up covering 24.94 km^2, forest covering 7.60 km^2, stony waste covering 19.14 km^2, forest plantations covering 1.25 sq km^2, fallow land covering 1.25 km^2, double-crop covering 7.15 km^2, and land without scrub covering 0.45 km^2 respectively.

Land use and land cover pattern of 2005: The kharif was the most major land use in the study area it covers an area of 142.82 km^2. The other two dominant land use classes were plantations and waterbodies. plantations covered an area of 65.21 km^2, waterbodies covered an area of 22.59 km^2. The scrubland is one of the dominant types of land cover in the study area, covering 8.94 km^2. Built-up land covers 31.10 km^2. In addition, scrub forests covered 7.60 km^2, Stony waste covered 19.68 km^2, and forest plantations covered 1.25 km^2 of the study area, while fallow land covered 9.62 km^2, double crops covered 9.94 km^2, and land without scrub covered 1.56 km^2.

Land use and land cover pattern of 2009: In 2009, kharif was the dominant land use class, covering an area of 137.26 km^2. Plantations cover a total area of 67.82 km^2, while water bodies cover 22.08 km^2. The scrubland covered an area of 8.45 km^2 of the study region. In the total area, approximately 36.47 km^2 area land is covered by built-up land. In addition, scrub forests covered 7.60 km^2, Stony waste covered 20.02 km^2, and forest plantations covered 1.25 km^2 of the study area, while fallow land covered 9.73 km^2, double crops covered 0.45 km^2, and land without scrub covered 1.35 km^2.

Land use and land cover pattern of 2012: The kharif crop is considered the most major land use type and it covered 130.24 km^2 in the study area. The scrub forest covers an area of 7.60 km^2. Moreover, the study area comprising 39.08 km^2 of built-up areas is the most common land-use category. The water bodies with an area of 21.94 km^2, and scrubland 8.40 km^2. The plantations covered 70.46 km^2 of the study area in 2012, becoming the second major land use category and a total area of 10.49 km^2 of fallow land is covered.

Land use and land cover pattern of 2015: The study revealed that built-up areas covered 39.08 km^2 in 2015, ranking third among the various land use categories. In addition, the scrub forest contributed an area of 7.60 km^2. The kharif covered 130.24 km^2 of the study area, making it the most prevalent type of land use. Although there were 5.28 km^2 of scrubland, it remained the most common land-use category. The water bodies covered a total area of 21.21 km^2, double crop covered an area of 5.46 km^2. Additionally, plantations consisted of 73.06 km^2 in the total area.

Land use and land cover pattern of 2020: In the year 2020, the most prevalent type of land use was the kharif crop, which covered 113.19 km^2 of the study area. The built-up area covered in total area of 60.59 km^2. Water bodies covered an area of 20.44 km^2, scrubland covered the was 4.15 km^2, and plantations covered an area of 79.22 km^2. However, the study area has an area of 8.91 km^2 of fallow land, which varies yearly due to irregular rainfall patterns, water shortages, and climate change. Further, the study area has 35 km^2 of double-crop land, which has been reduced due to inadequate water facilities. The stony waste is currently 20.44 km^2, and 1.06 km^2 of land without scrub was found. Nevertheless, the scrub forest is covered with an area of 7.60 km^2.

The Magnitude of Land Use and Land Cover Changes in the Tumkur City

From 2000 to 2020, the magnitude of change and annual change rate for different land use and land cover categories are shown in Table 4. In this study, agricultural land, scrubland, and water bodies have consistently decreased; on the other hand, built-up areas, and plantations, grow

Table 3: Land Use and Land Cover Change Statistics of Tumkur City from 2000 to 2020.

Class	Area in km^2 (2000)	Area in %	Area in km^2 (2005)	Area in %	Area in km^2 (2009)	Area in %	Area in km^2 (2012)	Area in %	Area in km^2 (2015)	Area in %	Area in km^2 (2020)	Area in %
Built-up Land	24.94	7.75	32.10	9.97	36.47	11.34	39.08	12.15	55.85	17.3	60.59	18.83
Double Crop	9.85	3.06	9.94	3.09	9.73	3.02	9.77	3.04	5.46	1.70	5.35	1.66
Fallow Land	7.15	2.22	9.62	2.99	9.70	2.94	10.77	3.34	8.41	2.61	8.91	2.77
Forest Plantation	1.25	0.41	1.25	0.39	1.25	0.39	1.25	0.39	1.25	0.39	1.25	0.39
Kharif Crop	154.46	48	143.23	44.52	137.26	42.67	130.72	40.63	122.51	38.07	113.19	35.18
Land Without Scrub	0.45	0.14	1.56	0.48	1.35	0.41	1.54	0.47	1.10	0.34	1.06	0.31
Plantation	61.57	19.14	65.21	20.27	67.82	21.08	70.54	21.92	73.06	22.7	79.22	24.62
Scrub Forest	7.60	2.36	7.60	2.36	7.60	2.36	7.60	2.36	7.60	2.36	7.60	2.37
Scrub Land	11.30	3.51	8.94	2.78	8.45	2.63	8.40	2.61	5.28	1.63	4.15	1.28
Stony Waste	19.14	5.95	19.68	6.11	20.02	6.22	20.09	6.25	20.06	6.23	20.00	6.23
Water Bodies	24.00	7.46	22.59	7.02	22.08	6.86	21.94	6.82	21.21	6.59	20.44	6.35
Total Area	321.66	100	321.66	100	321.66	100	321.66	100	321.66	100	321.66	100

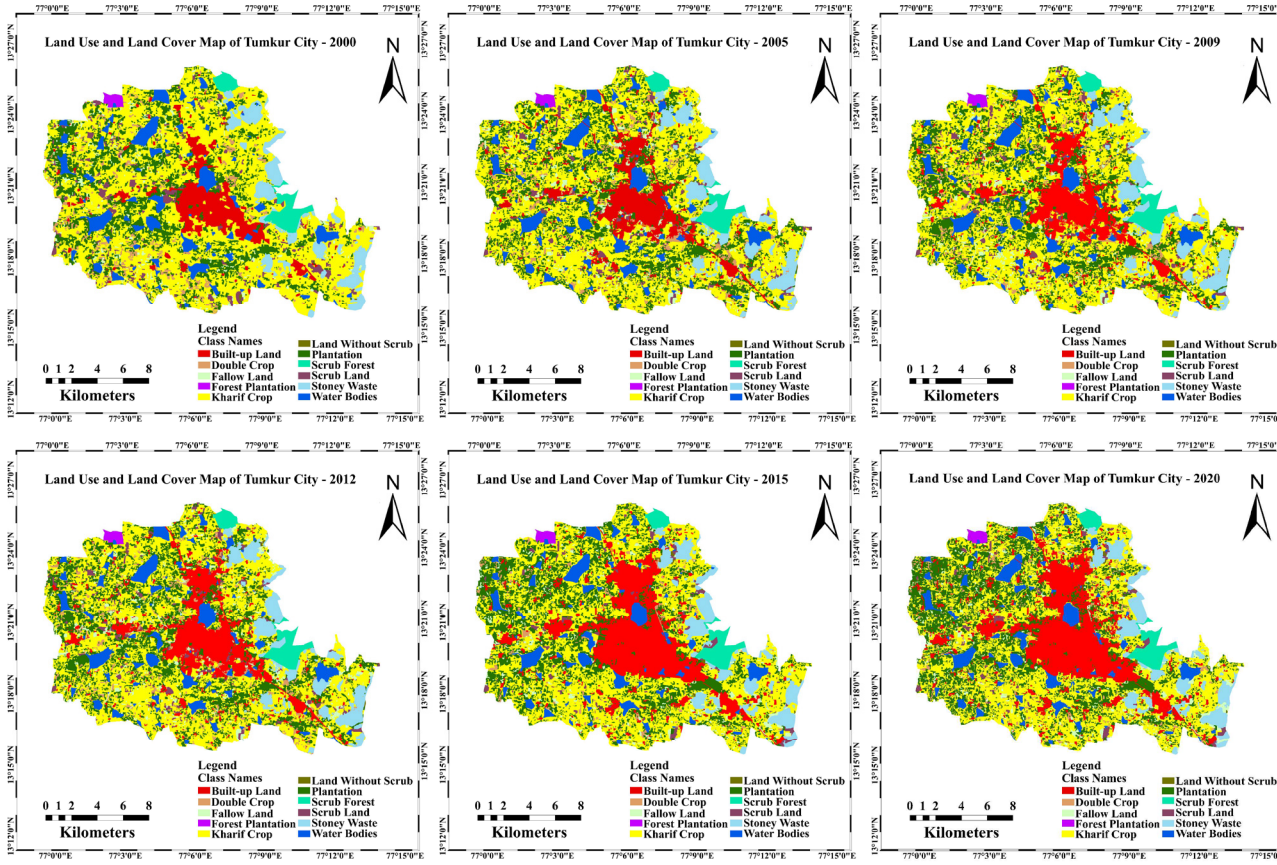

Fig. 4: Land use and land cover scenarios of Tumkur City in a) 2000, b) 2005, c) 2009, d) 2012, e) 2015, and f) 2020.

Table 4: Magnitude of change, percentage, and Annual Change Rate (ACR) of LULC in Tumkur city from 2000 to 2020.

Class Names	(2000-2005)			(2005-2009)			(2009-2012)			(2012-2015)			(2015-2020)		
	Area (km^2)	%	AC Rate (%)	Area (km^2)	%	AC Rate (%)	Area (km^2)	%	AC Rate (%)	Area (km^2)	%	AC Rate (%)	Area (km^2)	%	AC Rate (%)
Built-up Land	7.16	2.2	0.22	4.37	1.35	0.13	2.61	0.81	0.08	16.5	5.21	0.52	4.74	1.47	0.14
Double Crop	0.09	0.03	0.003	0.21	0.06	0.006	0.04	0.01	0.001	4.31	1.33	0.13	0.11	0.03	0.003
Fellow Land	2.47	0.7	0.076	0.08	0.02	0.002	1.07	0.33	0.03	2.36	0.73	0.07	0.53	0.15	0.01
Forest Plantation	0.01	0.05	0.005	0.02	0.006	0.0006	0.02	0.006	0.0006	0.02	0.006	0.00	0.03	0.009	0.0009
Kharif Crop	-11.2	3.4	0.349	-5.97	1.85	0.18	-6.52	2.02	0.20	-8.21	2.55	0.25	-9.32	2.89	0.28
Land Without Scrub	1.11	0.3	0.034	0.21	0.06	0.006	0.19	0.059	0.005	0.44	0.13	0.01	0.04	0.01	0.001
Plantation	3.64	1.1	0.113	2.61	0.81	0.081	2.72	0.84	0.08	2.52	0.78	0.07	6.16	1.91	0.191
Scrub Forest	0.02	0.04	0.004	0.03	0.009	0.0009	0.01	0.003	0.0003	0.02	0.006	0.0006	0.02	0.006	0.0006
Scrub Land	-2.36	0.7	0.073	0.498	0.15	0.015	0.05	0.015	0.001	3.12	0.96	0.09	1.13	0.35	0.03
Stony Waste	0.54	0.1	0.016	0.342	0.10	0.010	0.07	0.02	0.002	0.03	0.009	0.0009	0.05	0.01	0.001
Water Bodies	-1.41	0.4	0.043	-0.51	0.15	0.015	-0.14	0.043	0.004	-0.73	0.22	0.02	-0.77	0.23	0.02

continuously, and due to rock exposure stony waste has grown a little bit. It was found that the most considerable magnitude changes between 2000 and 2005 occurred in Kharif cropland (about 11.23 km^2) and built-up areas (7.16 $km^{2)}$. It has also been observed that significant magnitude changes between 2005 and 2009 occurred in the build-up area (1.35%) and plantation (2.61%); however, the Kharif crop decreased during this period. Furthermore, there has been vivid transmutation between 2009 and 2012, with build-up area (0.811%) followed by Kharif crops (2.026 %) and plantations (0.845%).

Furthermore, the annual changes in land area between the periods of 2012 and 2015 indicate a decrease in agricultural land (8.21 km^2) followed by water bodies (0.73 km^2) and double crop (4.31 km^2). In contrast, built-up areas (16.57 km^2), plantations (2.52 km^2), and fallow lands (2.36 km^2) have experienced annual increases. The magnitude results indicate that agricultural lands, scrublands, and waterbodies have consistently declined between 2015 and 2020. However, built-up areas, plantations, and fallow lands have continued to grow.

Land Use/Land Cover Degree Dynamic Index (LUCDDI) Analysis from 2000 to 2020

Land Use/Cover Degree Dynamic Index (LUCDDI) or Land Degree Dynamic Index (LDDI) values calculate the degree of land use dynamics, as shown in Table 5 and Fig. 5. The few land classes have low LDDI values that indicate a decline in the land area and few have positive values that imply gaining the area of land classes.

From 2000 to 2020, significant land changes have been witnessed, indicating that agricultural land, scrubland, and water bodies continually reduced; on the other hand, built-up areas, plantations, and stony waste experienced continuous growth. Additionally, LDDI indicates a high dynamic index value for the built-up area between 2000 and 2020, indicating that the built-up area expanded rapidly during the analysis period, while other types of land use, including agricultural areas, water bodies, and scrubland, remained with low LDDI values due to the rapid conversion of built-up. In contrast, built-up areas, plantations, and fallow land have continuously grown.

The Estimation of Land Transformation Matrix

Applying the different period land transformation matrix of LULC maps study to show the gains and losses in specific land use land cover class (Tables 6, 7, 8, 9, 10) Over the period between 2000 and 2020, large areas of agricultural land (154.2 km^2) will be converted into non-agriculture classes such as built-up land, plantations, and other classes

(113.33 km^2) due to the increase in the growth of major road networks like NH 48, NH 73, moreover, increase in the population growth, development activities carried out by government leads to boom the real estate of areas, growth of industrial areas in study area and quarrying activities. During the study period, the area of fallow land has extend due to proper water facilities. and economic stability and double crop have decreased consecutively due to inadequate water facilities, economic instability, and infertility of soil.

The built-up areas have increased and been encroached on by agricultural land, scrubland, and water bodies. This has influenced the expansion of urban areas due to an increase in better road networks like NH 48, NH 73, and state highways, development of industrial areas, and further, infrastructure activities developed by the Government like the development of roads, schools, colleges, and other commercial buildings. Urban regions have grown due to the population boom and the demand for housing, infrastructure, and commercial space. The scrubland is diminishing as it is converted into agricultural land, plantation, and built-up areas in a relatively short period; this is due to the development of industries, population growth, and economic stability. Moreover, due to the proper water facilities in areas and economic stability from 2000 to 2020, areas of plantation have increased and encroached by areas of water bodies, agricultural land, and scrubland. The few areas of water bodies are converted into agricultural land, plantations, and built-up areas like parks and residential areas due to the development of infrastructure development and the boom of real estate.

Quantification of Urban Sprawl using Shannon's Entropy

The Shannon entropy is often used to calibrate urban growth patterns' dispersion or compactness. Typically, Shannon's entropy ranges from 0 to log (n), with n representing the number of land use classes or categories. The entropy values higher than the log (n) value indicate the dispersion of urban areas in particular zones. Similarly, the entropy value is lower than log (n) which shows the compactness of urban areas in the particular zones. The Radar chart shows that between 2000 and 2020, the amount of entropy has increased irregularly (Fig. 6). The entropy values obtained are 0.999 in 2000, 0.998 in 2005, 0.980 in 2009, 0.997 in 2012, 1.010 in 2015 and 0.990 in 2020. Shannon's entropy for the year 2000 is 0.999, and the log n value of this is 0.9030, which means that the development of urban built-up is more towards the dispersion. Nevertheless, it was quite high for the year 2015, and the value of entropy is 1.010 and the log n value is 0.9030. New residential areas, a few infrastructure activities implemented by the smart city mission, and new industries development added during this period are the main reasons for the increase in dispersion between 2009 and 2020. Shannon's entropy values are calculated year-wise (Table 11) and each zone for all the two decades is presented in Table 12.

Table 5: Land Use Cover Dynamic Index of all classes (2000 to 2020).

Class	2000-2005	2005-2009	2009-2012	2012-2015	2015-2020
Built-up Land	5.74	3.40	2.38	14.30	2.82
Double Crop	0.18	-0.52	0.13	-14.70	-0.40
Fallow Land	6.90	0.20	3.67	-7.30	1.18
Forest Plantation	-0.03	-0.03	-0.02	0.053	-0.07
Kharif Crop	-2.42	-1.04	-1.58	-2.09	-1.52
Land Without Scrub	4.95	-3.36	4.69	-9.52	-0.72
Plantation	1.18	1.05	1.33	1.19	1.68
Scrub Forest	-0.02	0.02	0.02	0.02	-0.02
Scrub Land	-4.17	-3.70	-0.19	-12.30	-4.28
Stony Waste	0.56	0.43	0.11	-0.04	0.06
Water Bodies	-1.17	-0.56	-0.21	-1.10	-1.09

Interestingly the entropy values of all eight zones are close to log (n) values, indicating a high degree of dispersion. A residential area, an industrial area such as Hirehally, and national highways such as NH 48 and NH 73 in the East South East zone have a lower entropy value (1.020) than the West South East zone. From 2000, the index value increased gradually and reached 1.180 log (n) in 2014 compared to 1.0792 in 2000, indicating an increase in sprawl. The Values of entropy for the North and North East zone are 0.998, 0.99, 0.99, 1.035, 1.01, and 1.15 in 2000, 2005, 2009, 2012, 2015 and 2020, respectively. As a result, the present of three industrial areas has increased. According to TUDA Report from 2000 to 2020, TUDA Developed 80 Layouts in villages present in North North East zones. ENE zone records the least sprawl extent and intensity when compared with other zones due to the presence of hill areas and quarrying activities. The values of entropy for the West and North West zone are 0.98, 1.05, 1.07, 0.9915, 1.01, and 1.020 in 2000, 2005, 2009, 2012, 2015, and 2020 respectively. As a result, urban edge sprawl has spread further away from the urban cluster, although at a maximal rate, along such an axis. On the other hand, the SSE zone is undergoing maximum contemporary urban growth and haphazard sprawl patterns influenced by industry, while on the other hand, there are high concentrations of residential areas. The entropy value was 0.9923 in 2000, showing a gradual increase throughout, and reached an index value of 1.02 against 0.9030 log (n) in the year 2020. This is due to the impact of increasing residential areas and newly established developmental activities conducted by the smart city mission. From 2000 to 2020, the West South West zone has remained consistent over

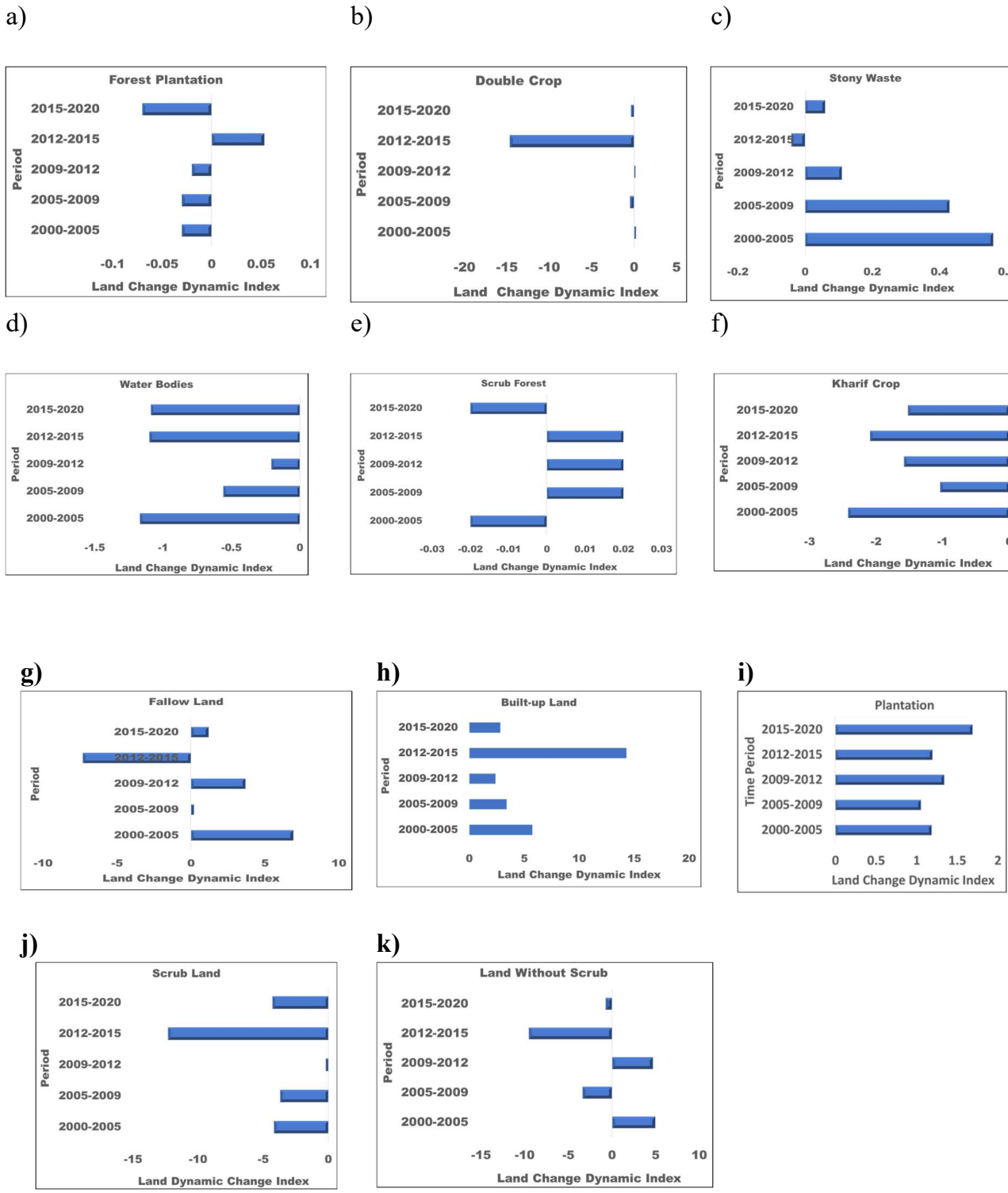

Fig. 5: Bar Graph showing the LDDI values of different land use and land cover classes from 2000 to 2020.

Table 6: Land Transformation Matrix of LULC of Tumkur City during 2000-2005.

LU/LC CLASSES		2000 in km^2												
		Builtup Land	Double Crop	Fallow Land	Forest Plantation	Kharif Crop	Land With-out Scrub	Plantation	Scrub Forest	Scrub Land	Stony Waste	Water Bodies	Total	Gain(+)
2005 in km^2	Builtup Land	16.6	0.4	0.2	0.0	10.4	0.0	1.7	0.0	0.4	0.1	0.2	32.1	13.4
	Double Crop	0.2	0.3	0.3	0.0	5.5	0.0	2.2	0.0	0.6	0.2	0.1	9.9	9.6
	Fellow Land	0.2	0.3	0.3	0.0	5.7	0.1	1.2	0.0	1.0	0.2	0.1	9.6	9.3
	Forest Plantation	0.0	0.0	0.0	1.2	0.0	0.0	0.0	0.0	0.0	0.0	0.0	1.3	0.1
	Kharif Crop	2.4	5.8	5.9	0.0	102.2	0.2	12.2	0.1	5.4	2.1	2.3	143.1	44.4
	Land Without Scrub	0.1	0.0	0.0	0.0	1.1	0.1	0.1	0.0	0.0	0.2	0.0	1.6	1.5
	Plantation	1.8	2.7	1.8	0.1	22.8	0.0	32.5	0.0	2.0	0.3	1.0	65.2	32.5
	Scrub Forest	0.0	0.0	0.0	0.0	0.0	0.0	0.0	7.5	0.0	0.0	0.0	7.6	0.1
	Scrub Land	0.5	0.2	0.3	0.0	4.9	0.1	0.9	0.0	1.5	0.5	0.1	8.9	7.5
	Stony Waste	0.0	0.0	0.1	0.0	3.6	0.0	0.1	0.0	0.3	15.3	0.0	19.6	4.1
	Water Bodies	0.2	0.1	0.1	0.0	1.5	0.0	0.5	0.0	0.1	0.2	20.0	22.6	2.6
	Total	25.0	9.8	7.1	1.3	154.2	0.5	61.5	7.6	11.3	19.1	24.0	**321.51**	
	Loss(-)	-6.9	-9.5	-6.7	-0.1	-55.9	-0.4	-28.9	-0.1	-9.8	-3.8	-3.8		

Table 7: Land Transformation Matrix of LULC of Tumkur City during 2005-2009.

LU/LC CLASS		2005 in km^2												
		Built-up Land	Double Crop	Fallow Land	Forest Plantation	Kharif Crop	Land Without Scrub	Plantation	Scrub Forest	Scrub Land	Stony Waste	Water Bodies	Total	Gain (+)
2009 in km^2	Builtup Land	30.54	0.43	0.56	0.00	3.73	0.04	0.98	0.00	0.02	0.00	0.15	36.47	5.91
	Double Crop	0.00	7.10	0.07	0.00	2.47	0.00	0.09	0.00	0.00	0.00	0.00	9.73	2.47
	Fellow Land	0.17	0.01	2.85	0.00	6.43	0.01	0.19	0.00	0.03	0.00	0.02	9.71	6.86
	Forest Plantation	0.00	0.00	0.00	1.26	0.00	0.00	0.01	0.00	0.00	0.00	0.00	1.27	0.01
	Kharif Crop	1.23	1.46	5.26	0.01	122.94	0.26	5.03	0.00	0.29	0.11	0.66	137.26	14.31
	Land Without Scrub	0.05	0.00	0.00	0.00	0.11	1.18	0.00	0.00		0.00	0.00	1.35	0.16
	Plantation	0.07	0.94	0.88	0.01	6.80	0.00	58.76	0.00	0.27	0.00	0.03	67.76	9.01
	Scrub Forest	0.00	0.00	0.00	0.00	0.00	0.00	0.00	7.60	0.00	0.00	0.00	7.60	0.01
	Scrub Land	0.00	0.00	0.00	0.00	0.07	0.00	0.00	0.00	8.32	0.00	0.06	8.45	0.13
	Stony Waste	0.00	0.00	0.00	0.00	0.37	0.07	0.01	0.00	0.00	19.56	0.00	20.02	0.08
	Water Bodies	0.04	0.01	0.00	0.0	0.24	0.00	0.13	0.00	0.00	0.00	21.66	22.08	0.42
	Total	32.11	9.95	9.62	1.28	143.16	1.57	65.21	7.61	8.93	19.68	22.59	**321.69**	
	Loss(-)	-1.56	-2.85	-6.77	-0.02	-20.22	-0.39	-6.44	-0.01	-0.29	-0.11	-0.92		

Table 8: Land Transformation Matrix of LULC of Tumkur City during 2009-2012.

LU/LC CLASS		2009 in km^2												
		Built-up Land	Double Crop	Fallow Land	Forest Plantation	Kharif Crop	Land Without Scrub	Plantation	Scrub Forest	Scrub Land	Stony Waste	Water Bodies	Total	Gain(+)
2012 in km^2	Builtup Land	36.33	0.13	0.03	0.00	2.09	0.00	0.43	0.00	0.00	0.00	0.07	39.08	2.75
	Double Crop	0.00	6.14	0.11	0.00	3.49	0.00	0.03	0.00	0.01	0.00	0.00	9.77	3.64
	Fellow Land	0.00	0.07	3.78	0.00	6.42	0.01	0.45	0.00	0.00	0.03	0.01	10.77	6.99
	Forest Plantation	0.00	0.00	0.00	1.24	0.01	0.01	0.00	0.00	0.00	0.00	0.00	1.26	0.01
	Kharif Crop	0.01	3.21	5.48	0.01	120.64	0.05	0.11	0.01	0.38	0.00	0.83	130.74	10.09
	Land Without Scrub	0.00	0.00	0.03	0.00	0.26	1.26	0.00	0.00	0.00	0.00	0.00	1.55	0.29
	Plantation	0.01	0.13	0.25	0.00	3.21	0.02	66.65	0.00	0.11	0.01	0.08	70.48	3.22
	Scrub Forest	0.00	0.00	0.00	0.00	0.00	0.00	0.00	7.60	0.00	0.01	0.00	7.61	0.01
	Scrub Land	0.00	0.00	0.00	0.00	0.48	0.00	0.00	0.00	7.93	0.00	0.00	8.40	0.48
	Stony Waste	0.00	0.04	0.03	0.00	0.04	0.00	0.00	0.00	0.00	19.97	0.01	20.09	0.12
	Water Bodies	0.12	0.01	0.01	0.00	0.63	0.00	0.08	0.00	0.02	0.00	21.06	21.94	0.87
	Total	36.48	9.73	9.71	1.25	137.26	1.36	67.76	7.61	8.45	20.03	22.07	**321.69**	
	Loss (-)	-0.13	-3.59	-5.94	-0.01	-16.63	-0.08	-1.10	-0.01	-0.52	-0.05	-1.01		

Table 9: Land Transformation Matrix of LULC of Tumkur City during 2012-2015.

LU/LC CLASS		2012 in km^2												
		Builtup Land	Double Crop	Fallow Land	Forest Plantation	Kharif Crop	Land Without Scrub	Plantation	Scrub Forest	Scrub Land	Stony Waste	Water Bodies	Total	Gain (+)
2015 in km^2	Builtup Land	34.47	1.60	1.65	0.00	9.58	0.25	6.19	0.00	1.37	0.27	0.48	55.86	21.39
	Double Crop	0.17	0.19	0.30	0.00	3.31	0.02	1.27	0.00	0.13	0.01	0.05	5.45	5.26
	Fellow Land	0.25	0.52	0.47	0.02	4.73	0.13	1.67	0.00	0.29	0.23	0.08	8.39	7.92
	Forest Plantation	0.00	0.00	0.00	1.20	0.05	0.00	0.01	0.00	0.00	0.00	0.00	1.26	0.06
	Kharif Crop	2.08	4.23	5.01	0.01	82.71	0.67	21.80	0.01	3.00	2.16	1.65	123.35	40.62
	Land Without Scrub	0.01	0.01	0.08	0.00	0.50	0.12	0.07	0.00	0.05	0.25	0.00	1.10	2.07
	Plantation	1.80	2.81	2.59	0.00	26.01	0.11	37.85	0.05	1.17	0.21	0.50	73.12	35.25
	Scrub Forest	0.00	0.00	0.00	0.00	0.01	0.00	0.00	7.55	0.00	0.04	0.00	7.61	-.05
	Scrub Land	0.09	0.09	0.33	0.00	1.50	0.01	0.43	0.01	1.96	0.76	0.09	5.28	3.31
	Stony Waste	0.10	0.24	0.30	0.00	2.07	0.22	0.54	0.03	0.34	16.11	0.06	20.02	3.90
	Water Bodies	0.09	0.07	0.12	0.02	1.12	0.01	0.62	0.00	0.09	0.03	19.02	21.18	2.15
	Total	39.08	9.76	10.86	1.25	131.60	1.54	70.46	7.66	8.42	20.07	21.93	**321.69**	
	Loss (-)	-4.59	-9.57	-10.30	-0.03	-48.88	-1.42	-32.60	-0.07	-6.45	-3.96	-2.91		

Table 10: Land Transformation Matrix of LULC of Tumkur City during 2015-2020.

LU/LC CLASS		2015 in km2												
		Builtup Land	Double Crop	Fallow Land	Forest Plantation	Kharif Crop	Land Without Scrub	Plantation	Scrub Forest	Scrub Land	Stony Waste	Water Bodies	Total	Gain (+)
2020 in km^2	Builtup Land	54.97	0.23	0.25	0.00	4.02	0.06	0.549	0.000	0.182	0.047	0.258	60.58	5.61
	Double Crop	0.030	3.57	0.60	0.00	0.58	0.00	0.417	0.000	0.105	0.000	0.027	5.354	1.77
	Fellow Land	0.000	0.794	6.20	0.000	0.894	0.00	0.535	0.000	0.429	0.035	0.018	8.908	2.70
	Forest Plantation	0.000	0.000	0.009	1.195	0.010	0.00	0.003	0.000	0.000	0.000	0.043	1.259	0.04
	Kharif Crop	0.262	0.260	0.38	0.034	107.83	0.00	2.669	0.000	0.681	0.344	0.742	113.21	5.37
	Land Wit hout Scrub	0.012	0.000	0.00	0.00	0.00	0.99	0.00	0.00	0.00	0.00	0.00	1.012	0.01
	Plantation	0.502	0.490	0.605	0.030	8.38	0.00	68.706	0.000	0.259	0.015	0.235	79.22	10.51
	Scrub Forest	0.000	0.000	0.000	0.000	0.08	0.00	0.000	7.54	0.00	0.00	0.00	7.63	0.089
	Scrub Land	0.00	0.100	0.294	0.000	0.01	0.037	0.126	0.000	3.918	0.002	0.016	4.51	0.59
	Stony Waste	0.00	0.00	0.038	0.00	0.27	0.00	0.00	0.033	0.070	19.61	0.020	20.05	0.43
	Water Bodies	0.070	0.004	0.019	0.000	0.39	0.000	0.056	0.000	0.041	0.000	19.851	20.43	0.58
	Total	55.851	5.458	8.415	1.260	122.5	1.105	73.06	7.581	5.68	20.06	21.20	**321.69**	
	Loss (-)	-0.876	-1.88	-2.21	-0.03	-14.6	-1.21	-4.35	-0.03	-1.74	-0.443	-1.35		

the temporal period, with minimal fluctuations. Compared to other zones, the WSW zone recorded the least amount and severity of sprawl. From 2000 to 2020 few areas like Hegere and Malasadra villages have of new residential areas developed. But future WSW developed very rigorously due to the National Highway projects proposal going on and some developmental activities implemented by Smart city mission by the central government. The NNW zone is facing the maximum expansion of built-up areas and a haphazard sprawl pattern greatly influenced by industries, and new residential areas present on the adjacent sides of highways and villages. The study discloses that built-up area growth and land use patterns have shifted, and a complex pattern of urban sprawl has developed in various directions. Figs. 7 and 8 show the Urban expansion Map and integrated map of Tumkur City.

Monitoring Urban Expansion Intensity Index (UEII)

A UEII describes the nature of the urban expansion of Tumkur City; the zone-wise statistics are presented in Table 13. Between 2000 and 2020, there was an urban expansion intensity index of 0.11 at the lowest point and 2.60 at the highest point, which is considered a high rate of urban expansion. Between 2000 and 2005, the overall study area had an expansion intensity index of 0.53, which is considered moderate for urban expansion. Furthermore, between 2009 and 2012, the UEII increased dramatically from 0.23 to 1.77 from 2012-2015; this rapid increase in UEII indicates an increased likelihood of urban sprawl occurring as a result of various infrastructure projects initiated by the government, an increase in industries, and an increase in population. In the period (2000 to 2020), the highest UEIIs have been observed in zones with built-up fringe areas and high sprawled urban expansion rates. In the period 2005-2009, urban land in Tumkur City began dispersing to the east, north, west, and south-south west, but in the period 2012-2020, urban land began to disperse almost in all directions (i.e. south, southeast, west, and southwest). Fig. 9 shows that the UEII values in different zones have increased in different directions from 2000 to 2020. It is evident from the significant increase in UEII that urban sprawl is becoming more prevalent. It implies that there was notable urban sprawl during this time, reflecting the spread of urban regions into previously undeveloped or rural areas.

Monitoring of Urban Growth using Regression Analysis

Spatio-temporal pattern of built-up density: It was determined the built-up density in each spatial unit of Tumkur city to identify the density of urbanized areas and their spatio-temporal variation. To identify the density of

Table 11: Shannon's entropy index of Tumkur city (zone-wise).

Year	Built-up Area (sq. km)	Entropy Value	Log (n)
2000	24.94	0.999	0.9030
2005	32.10	0.998	0.9030
2009	36.47	0.980	0.9030
2012	39.08	0.997	0.9030
2015	55.85	1.010	0.9030
2020	60.59	0.990	0.9030

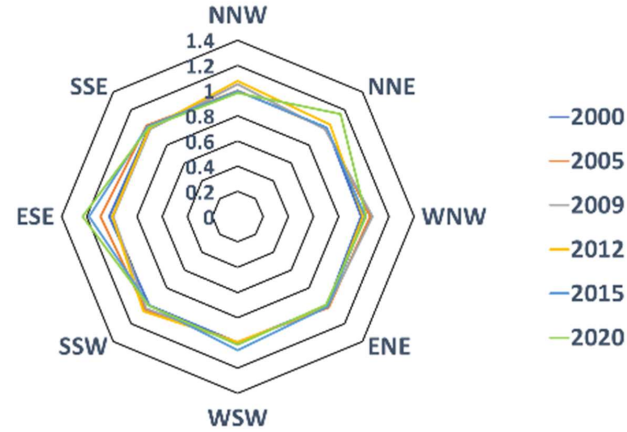

Fig. 6: Radar map depicting zone-specific urban sprawl patterns throughout time.

urbanized areas and their spatiotemporal variation, it was determined the built-up density within each spatial unit of Tumkur City. Built-up density in all zones of Tumkur city areas was very low in 2000 and continued to increase in 2020 has been observed. It is estimated that the built-up density in zones like the NNE, ESE, and SSW will be higher in 2020 than in 2000 (Tables 14 and 15). The TUDA is constructing large residential and industrial developments in these areas, such as Hirehalli, Satyamagala, Antharasanahally Phase 1 and Antharasanahally Phase 2. Some industrial estates have been developed by KIADB along NH 4 in the northern part of the city since 2009. These include Sathyamagala, Lingapura, and Antharasanahally. According to SSE statistics, built-up density has increased from 0.0694 to 0.2009 between 2000 and 2020, indicating that the development of urban built-up is moving toward dispersion. In the WNW zone, which is essentially an NH 73, a new residential area and lesser built-up density value (0.7754) in 0.0845, the index value progressively increased to reach 0.1602 in 2020, indicating an increase in sprawl. During 2000-2020, the built-up density in the WSW zone increased considerably, but compared with other zones, it is still relatively low. As for the ENE zone, the built-up density value is higher, primarily due to the highways, such as NH 48, connecting major cities within the country. The NNW zone is experiencing rapid urban

Table 12: Shannon Entropy values of different zones from 2000 to 2020.

Year	Zones							
	NNW	NNE	WNW	ENE	WSW	SSW	ESE	SSE
2000	0.999	0.998	0.98	0.995	0.998	0.9923	1.020	0.996
2005	1	0.99	1.05	0.990	0.9915	1.04	1.09	1.025
2009	1.05	0.98	1.07	0.991	0.98	1.03	0.99	0.98
2012	1.075	1.035	0.9915	0.992	0.992	1.058	0.995	0.991
2015	0.9955	0.998	1.01	0.998	0.997	1.098	1.180	1.015
2020	0.98	1.15	1.020	0.99	0.998	1	1.23	1

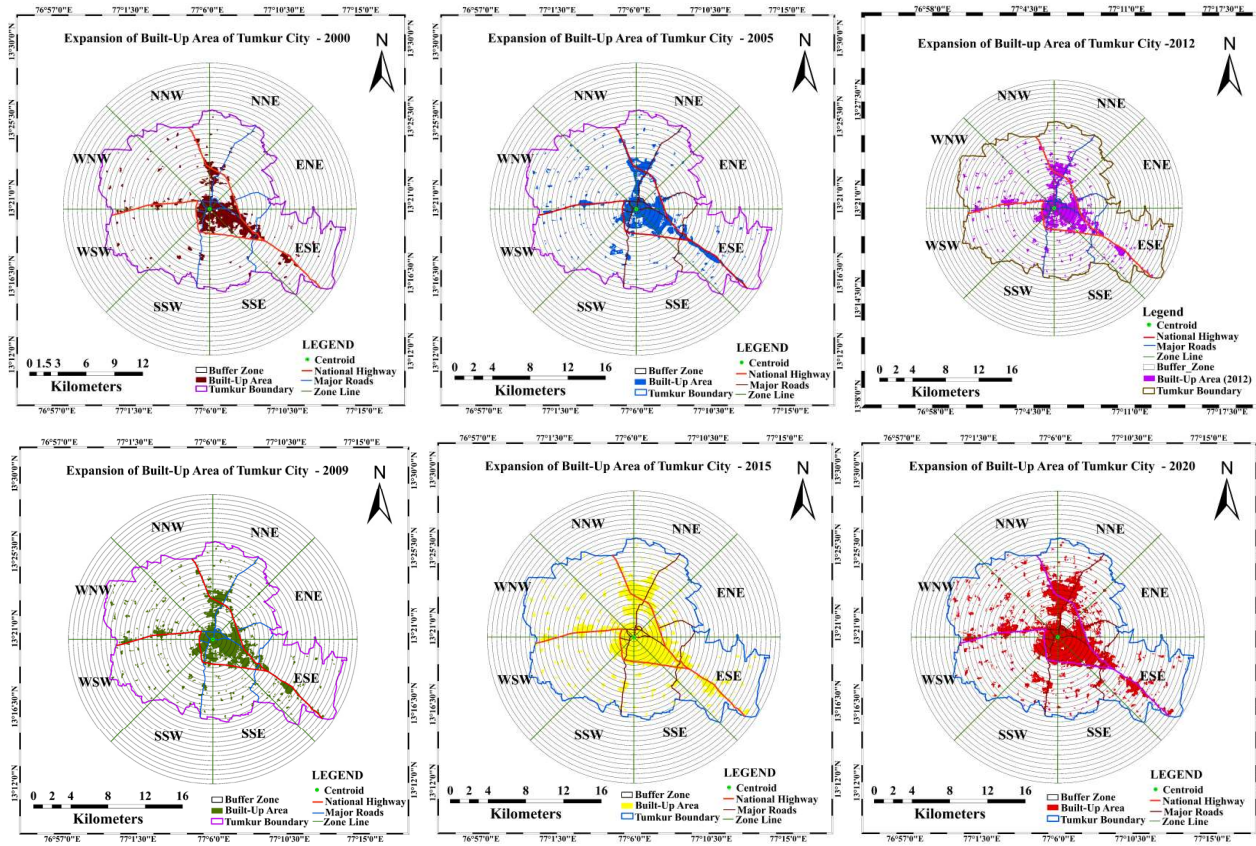

Fig. 7: Urban expansion Map of Tumkur City in (a) 2000, (b) 2005, (c) 2009 (d) 2012, (e) 2015, (f) 2020.

growth and a haphazard sprawl pattern greatly influenced by National Highway 48. From 2000 to 2020, TUDA has developed a wide range of residential areas.

Annual Urban Spatial Expansion Index (AUSEI)

The higher values of AUSEI show the development of built-up areas increased and lower values are an indication of a decrease in the growth of built-up areas during the period. The AUSEI index is useful for determining the geographical pattern of urban growth at a given period. From 2000-2012, the urban expansion index of all zones showed a slight variation in growth, whereas from 2012-2015, the value of the urban expansion index increased (Table 16). In the period 2012 to 2015, the highest rate of urban expansion was recorded in areas and the presence of new residential areas in the core of the city and outside of the city. As a consequence of the sudden increase in urban values during 2012, heavily influenced by National Highway 48 on the one hand and the numerous residential areas developed by TUDA from 2000 to 2020 on the other, the urban expansion values of the WNW zone declined from 2000 to 2012. Heggere is located near the National Highway 76. Some wards, such as Bheemasadra

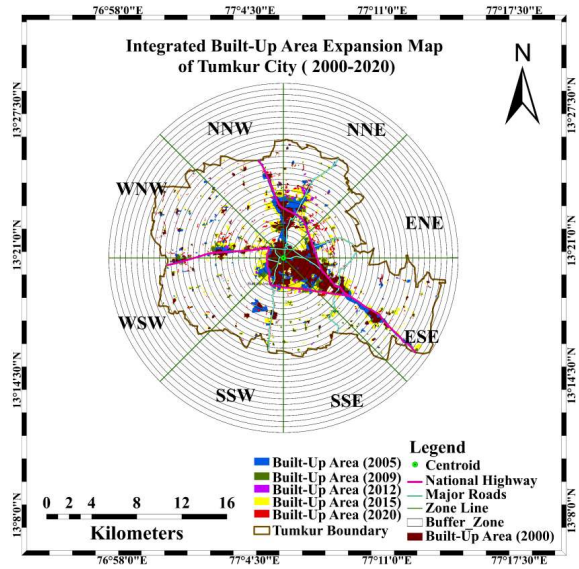

Fig. 8: Integrated Urban Expansion Map of the Tumkur City from 2000 to 2020.

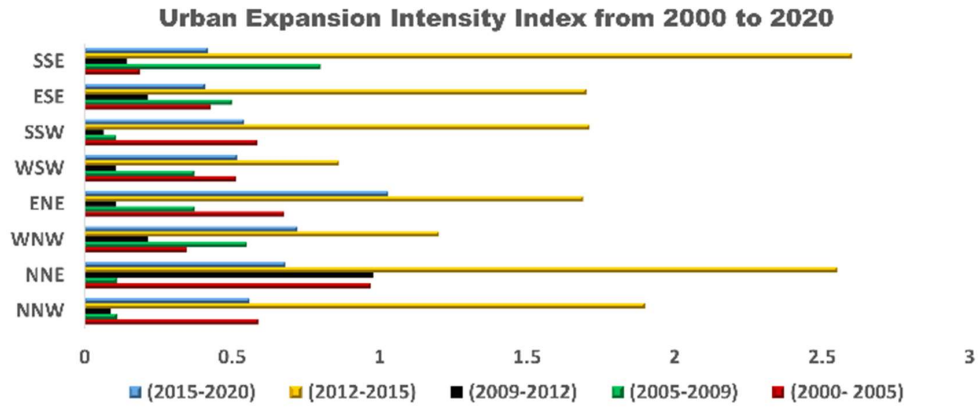

Fig. 9: Bar chart of UEII from 2000 to 2020.

Table 13: Urban Expansion Intensity Index of all zones (2000 to 2020).

Zones	Year				
	2000-2005	2005-2009	2009-2012	2012-2015	2015-2020
NNW	0.588	0.11	0.0875	1.90	0.56
NNE	0.97	0.1098	0.9796	2.55	0.68
WNW	0.348	0.5492	0.2160	1.20	0.723
ENE	0.676	0.373	0.107	1.69	1.030
WSW	0.5147	0.3712	0.1049	0.863	0.5164
SSW	0.585	0.108	0.064	1.71	0.54
ESE	0.4272	0.50130	0.2131	1.70	0.4097
SSE	0.1869	0.80	0.14468	2.60	0.4178
Total	0.5367	0.3653	0.2395	1.77	0.912

and KHB Colony, were influenced by the expansion of the urban area. From 2000 to 2012, urban expansion values in zones such as ESE, SSW, and NNE were very low. Since 2012, urban expansion values have increased as an output of the progression of industrial areas and several infrastructure projects developed by Smart City Mission. Some wards such as Bheemasadra and KHB Colony, were influenced by the expansion of the urban area. From 2000 to 2012, urban expansion values in zones such as ESE, SSW, and NNE were very low. Since 2012, urban expansion values have increased due to the development of industrial areas and some infrastructure projects developed by Smart City Mission. During the period 2000 to 2020, the development of better road networks by the government and economic progress has led to a rise in settlements in rural villages in the ESE,

Table 14: The Built-up areas of different zones in Tumkur City.

Zones	Total Area	2000	2005	2009	2012	2015	2020
NNW	38.08	2.505	3.626	3.56	3.89	6.08	7.158
NNE	37.77	3.195	5.034	5.18	6.31	9.20	10.44
WNW	54	2.352	3.29	4.39	4.74	6.70	8.654
ENE	21.74	1.972	2.75	3.03	3.10	4.208	5.328
WSW	44.46	1.338	2.460	3.12	3.26	4.412	5.56
SSW	25.92	2.35	3.113	2.98	3.05	4.433	5.13
ESE	68.82	9.19	10.66	12.04	11.95	15.125	16.53
SSE	29.95	2.08	2.36	3.32	3.45	5.848	6.019

Table 15: Built-up Density of different zones in Tumkur City areas.

Zones	2000	2005	2009	2012	2015	2020
NNW	0.0658	0.0952	0.0991	0.1021	0.1596	0.1879
NNE	0.0845	0.1332	0.1378	0.1670	0.2435	0.2764
WNW	0.0435	0.0609	0.0814	0.0877	0.1240	0.1602
ENE	0.0907	0.1244	0.1392	0.1425	0.1935	0.2450
WSW	0.0300	0.0553	0.0701	0.0733	0.0992	0.1250
SSW	0.0906	0.1206	0.1114	0.1176	0.1710	0.1981
ESE	0.1335	0.1548	0.1724	0.1656	0.2197	0.2401
SSE	0.0694	0.0787	0.1108	0.1151	0.1952	0.2009

SSW, and NNE zones such as Machenahalli, Basavapatna, Maraluru, Singanahalli, Arakere, Yallapura, etc. Between 2000 and 2012, the Urban Expansion Index value varied in the SSW zone, but between 2012 and 2020, it increased. This indicated a rise in the growth of urban areas due to the few residential layouts developed by TUDA and the few infrastructure projects developed by Smart City Mission's Central Government.

As a result of urban expansion values varying from 2000 to 2012 in the few zones like WNW, NNW, SSE, and WSW, large residential areas are present, built-up areas are developed along national and state highways, and industrial areas and industrial estates are developed by the Karnataka Industrial Area Development Board (KIADB). Expansion values have increased between 2012 and 2015 but have slowed down since 2015. This indicated that the expansion of built-up areas is slow compared to 2000 to 2015, but the built-up area is expanded.

Annual built-up change index (ABUCI): The yearly rate of change in built-up areas was established by calculating the total built-up area in high-density and low-density classes each year and detecting the change over successive years (Table 17). The pattern of the annual change rate in Tumkur city is that, as a whole, the built-up areas of the rural have not experienced a significant rate of annual built-up change during the period from 2000 to 2012. In contrast, after 2012, the zones, especially ESE, SSW, and NNE experienced annual change at a faster rate. The study reveals the presence of industrial areas such as Hirehalli, Antharasanahally Phase 1 and Antharasanahally Phase 2, Satyamagala, and the presence of new residential areas both within and outside the city. Between 2012 and 2015, the real estate market experienced a boom, which affected the rate of change annually. The rate of annual built-up change in the WNW zone was only 18.8 % in 2000–2005, which increased about three times (65.38 %) in the later period, 2012–2015. This zone experienced the highest rate of change in built-up areas, followed by SSE and NNWUrbanization is caused by the conversion of agricultural land, scrubland, and other land-use and land-cover types. The study shows that outside of the center region, there is lots of prospective space for future development of urban growth.

In contrast, core regions are often packed, with little or no possibility for additional expansion, resulting in a spatial pattern of built-up change over time. In 2000, the rate of change in the NNW zone was estimated to be 22 %. However, the rate of change is three times greater (72.6 %) between 2012 and 2015. This shows that urban areas are expanded and influenced by the boom of real estate in those areas. Compared to other zones such as NNW, NNE, and ESE, the rate of change of built-up in ENE, SSE, and WSW is low. This indicated that the built-up is expanding in city

areas and a few villages like Hettenahalli, Kaidala, etc. In rural areas, settlements increased as a result of better road connectivity between cities and rural areas, and because of the presence of highways, real estate booms occurred between 2010 and 2020.

Assessing Interrelationship among BD, AUSEI and ABUCI: The correlation coefficients of the Built-up Density index (BD), Annual Urban Spatial Expansion Index (AUSEI), and Annual Built-up Change Index (ABUCI) were estimated by regression analysis to identify the interrelationships among them. It is evident from the correlation between the urban expansion index and the annual rate of change in the built-up area that they are well correlated and have a significant positive relationship. There is a strong correlation between the ABUCI and AUSEI since areas with a high AUSEI are also experiencing high rates of annual change in built-up areas, and vice versa. In 2012–2015, there was a very strong correlation between the two variables. The correlation between built-up density and urban expansion index shows a very strong negative correlation with a significant correlation coefficient (Fig. 10). According to the results, R^2 was 0.5258,0.5027,0.5516, 0.5225, and 0.622 for the various periods. The data indicate that areas with a high density of built-up areas have not expanded as much. In contrast, urban expansion has occurred primarily in areas with a low density of built-up areas. AUSEI has been comparatively higher in these areas since they have not yet been fully developed and still have sufficient lands for potential growth. In comparing the relationship between built-up density and the annual rate of change in a built-up area, it was discovered that there was a high negative correlation between the two variables. For 2000, 2005, 2009, 2012, 2015, and 2020, with an R^2 value of 0.560, 0.5439, 0.6223, 0.5368 and 0.5267, respectively. In high-density regions, there were no notable changes; conversely, in low-density areas, there were significant alterations. On the other hand, the abundance of vacant land made low-density built-up regions ideal for conversion. Land-use land-cover dynamics in core and peri-urban areas are important for the development of smart cities, particularly in the planning of sustainable land use. For the implementation of smart city missions, it is necessary to consider information regarding spatio-temporal variations in urban growth. Interrelationship results revealed that rapid urban growth experienced in the study area leads increase in some consequences.

CONCLUSION

From 2000 to 2020, geospatial techniques were used to analyze Tumkur City's urban land use and land cover changes and, according to the change magnitudes, the Land Use/Cover Degree Dynamic Index and LULC transformation matrix revealed that increased large areas of built-up land were contributed by kharif crop, scrubland and waterbodies, and increased plantations contributed by kharif crop and

Table 16: The AUSEI values of different zones in Tumkur City (2000-2020).

Zones	Year				
	2000- 2005	2005-2009	2009-2012	2012-2015	2015-2020
NNW	6.1787	0.2457	1.4685	12.01	6.1787
NNE	7.305	0.70	5.96	10.47	2.37
WNW	5.7142	6.26	2.4613	9.75	4.5158
ENE	5.39	2.68	0.7526	9.912	4.120
WSW	9.12	5.2884	1.431	9.761	4.129
SSW	4.90	-0.9416	0.546	10.399	2.73
ESE	2.748	2.86	0.1377	17.107	2.830

Table 17: The ABUCI values of different zones in Tumkur City (2000-2020).

Zones	Year				
	2000- 2005	2005-2009	2009-2012	2012-2015	2015-2020
NNW	22	4.35	3.33	72.6	21.4
NNE	36	3.65	37.66	96.33	24.8
WNW	18.8	27.5	11.66	65.38	39.1
ENE	14.6	8.25	3.33	35.93	22.4
WSW	22.6	16.5	4.66	39	23
SSW	15.2	3.15	2.33	46	14
ESE	5.6	24.13	4.33	79.66	3.58

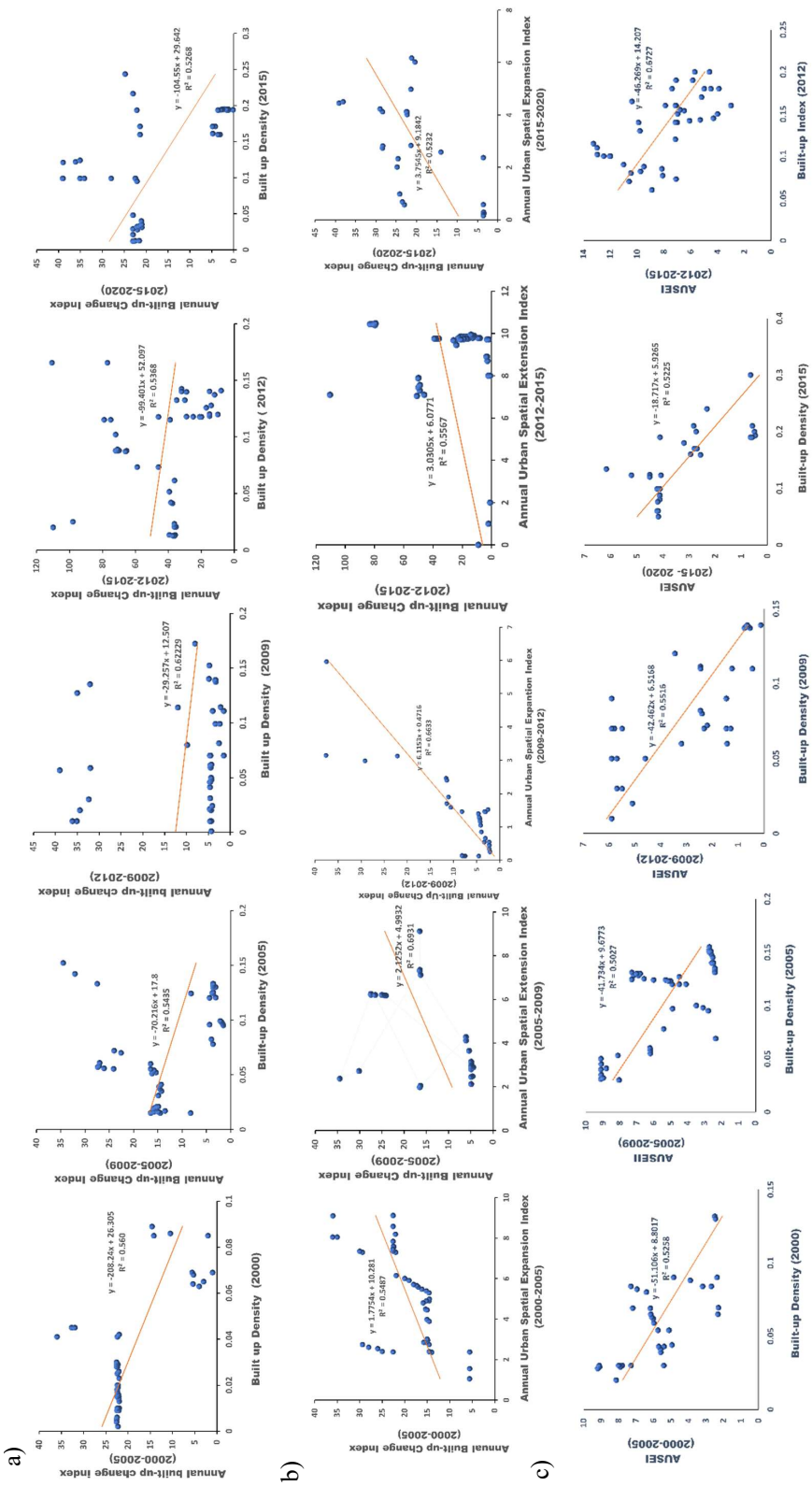

Fig. 10: Interrelationships Scatter plot among Built-up Density and ABUCI (**a**), ABUCI and AUSEI (**b**), Built-up Density and ABUCI (**c**)

scrubland. Further, the study focused on determining the built-up land patterns using urban sprawl and urban growth analysis by deriving various indices. The derived entropy values greater than the Log (n) values in Shannon Entropy indicate large built-up areas are expanding in the zones such as WNW, NNE, ENE, and ESE due to the development of the road network system, population growth, and industrial growth, which shows an increase in the urban sprawl. Further, the urban growth analysis carried out by the UEII statistics shows a high level of urban expansion after 2009, and the correlation between built-up density, ABUCI, and ASEI results indicated the expansion of urban areas, mainly in the center and industrial regions of the city. The study's overall findings have demonstrated how beneficial it is to utilize geospatial technology to investigate the degree and stress of urbanization on land and water resources. The conversion of kharif into plantations built-up land indicated increased food insecurity due to the growth of real estate. Further, the present study's findings will provide to understanding of land use dynamics, urban sprawl, urban growth analysis, and future projections, as well as provide crucial information for decision-making and urban planning processes to the urban planners, supporting the improvement of policy implications on supportable land use management and guiding strategies for appropriate urban development.

REFERENCES

Antipova, A., Momeni, E. and Banai, R., 2022. Analysis of Urban Sprawl and Blight Using Shannon Entropy Index: A Case Study of Memphis, Tennessee. In *Advances in Urbanism, Smart Cities, and Sustainability* (pp. 322-299). CRC Press. http://dx.doi.org/21-9781003126195/10.1201.

Bhatta, B., Saraswati, S. and Bandyopadhyay, D., 2010. Quantifying the degree-of-freedom, degree-of-sprawl, and degree-of-goodness of urban growth from remote sensing data. *Applied Geography*, 30(1), pp. 96-111. https://doi.org/10.1016/j.apgeog.2009.08.001.

Brown, D.G., Pijanowski, B.C. and Duh, J.D., 2000. Modeling the relationships between land use and land cover on private lands in the Upper Midwest, USA. *Journal of Environmental Management*, 59(4), pp. 247-263. https://10.12691/aees-1-6-5.

Bunyangha, J., Majaliwa, M.J., Muthumbi, A.W., Gichuki, N.N. and Egeru, A., 2021. Past and future land use/land cover changes from multi-temporal Landsat imagery in Mpologoma catchment, eastern Uganda. *The Egyptian Journal of Remote Sensing and Space Science*, 24(3), pp. 675-685. http://dx.doi.org/10.1016/j.ejrs.2021.02.003.

Burgalassi, D. and Luzzati, T., 2015. Urban spatial structure and environmental emissions: A survey of the literature and some empirical evidence for Italian NUTS 3 regions. *Cities*, 49, pp. 134-148. https://doi.org/10.1016/j.cities.2015.07.008.

Dadras, M., Shafri, H.Z., Ahmad, N., Pradhan, B. and Safarpour, S., 2015. Spatio-temporal analysis of urban growth from remote sensing data in Bandar Abbas city, Iran. *The Egyptian Journal of Remote Sensing and Space Science*, 18(1), pp. 35-52. http://dx.doi.org/10.1016/j.ejrs.2015.03.005.

Dahly, D.L. and Adair, L.S., 2007. Quantifying the urban environment: a scale measure of urbanicity outperforms the urban–rural dichotomy. *Social Science & Medicine*, 64(7), pp. 1407-1419. https://psycnet.apa.org/doi/10.1016/j.socscimed.2006.11.019.

Deng, J.S., Wang, K., Deng, Y.H. and Qi, G.J., 2008. PCA-based land-use change detection and analysis using multitemporal and multisensor satellite data. *International Journal of Remote Sensing*, 29(16), pp. 4823-4838. http://dx.doi.org/10.1080/01431160801950162.

Didier, S., Peyroux, E. and Morange, M., 2012. The spreading of the city improvement district model in Johannesburg and Cape Town: urban regeneration and the neoliberal agenda in South Africa. *International Journal of Urban and Regional Research*, 36(5), pp. 915-935. DOI:10.1111/j.1468-2427.2012.01136.

Dijoo, Z.K., 2021. Urban heat island effect concept and its assessment using satellite-based remote sensing data. *Geographic Information Science for Land Resource Management*, pp. 81-98. https://doi.org/10.1002/9781119786375.ch5.

Dutta, D., Rahman, A., Paul, S.K. and Kundu, A., 2019. Changing pattern of urban landscape and its effect on land surface temperature in and around Delhi. *Environmental monitoring and assessment*, *191*, pp.1-15.

Dutta, D., Rahman, A., Paul, S.K. and Kundu, A., 2020. Estimating urban growth in peri-urban areas and its interrelationships with built-up density using earth observation datasets. *The Annals of Regional Science*, 65, pp. 67-82. https://link.springer.com/article/10.1007/s00168-020-00974-8.

Grekousis, G., Manetos, P. and Photis, Y.N., 2013. Modeling urban evolution using neural networks, fuzzy logic and GIS: The case of the Athens metropolitan area. *Cities*, 30, pp. 193-203. https://doi.org/10.1016/j.cities.2012.03.006.

Grodach, C. and Guerra-Tao, N., 2022. Industrial lands, equity, and economic diversity: a comparative study of planned employment areas in Melbourne, Australia. *Urban Research & Practice*, pp. 1-17. https://doi.org/10.1080/17535069.2022.2080583.

Haque, M.I. and Basak, R., 2017. Land cover change detection using GIS and remote sensing techniques: A spatio-temporal study on Tanguar Haor, Sunamganj, Bangladesh. *The Egyptian Journal of Remote Sensing and Space Science*, 20(2), pp. 251-263. http://dx.doi.org/10.1016/j.ejrs.2016.12.003

Herold, M., Couclelis, H. and Clarke, K.C., 2005. The role of spatial metrics in the analysis and modeling of urban land use change. *Computers, Environment and Urban Systems*, 29(4), pp.369-399. http://dx.doi.org/10.1016/j.compenvurbsys.2003.12.001.

Hong, Z., Hailin, L. and Zhen, C., 2011. Analysis of land use dynamic change and its impact on the water environment in Yunnan plateau lake area—A case study of the Dianchi lake drainage area. *Procedia Environmental Sciences*, 10, pp.2709-2717.

Jaad, A. and Abdelghany, K., 2021. The story of five MENA cities: Urban growth prediction modeling using remote sensing and video analytics. *Cities*, *118*, p.103393.

Ji, W., Ma, J., Twibell, R.W. and Underhill, K., 2006. Characterizing urban sprawl using multi-stage remote sensing images and landscape metrics. *Computers, Environment and Urban Systems*, 30(6), pp.861-879. https://doi.org/10.1016/j.compenvurbsys.2005.09.002.

Kasraian, D., Maat, K. and van Wee, B., 2019. The impact of urban proximity, transport accessibility and policy on urban growth: A longitudinal analysis over five decades. *Environment and Planning B: Urban Analytics and City Science*, 46(6), pp.1000-1017. http://dx.doi.org/10.1177/2399808317740355.

Khan, R. and Jhariya, D.C., 2018. Assessment of land-use and land-cover change and its impact on groundwater quality using remote sensing and GIS techniques in Raipur City, Chhattisgarh, India. *Journal of the Geological Society of India*, 92, pp.59-66. https://doi.org/10.1007/s12594-018-0953-3.

Kim, C., 2016. Land use classification and land use change analysis using satellite images in Lombok Island, Indonesia. *Forest Science and Technology*, 12(4), pp.183-191. https://doi.org/10.1080/21580103.2016.1147498.

Kindu, M., Schneider, T., Teketay, D. and Knoke, T., 2013. Land use/land cover change analysis using object-based classification approach in Munessa-Shashemene landscape of the Ethiopian highlands. *Remote Sensing*, 5(5), pp.2411-2435. http://dx.doi.org/10.3390/rs5052411.

Lambin, E.F., Turner, B.L., Geist, H.J., Agbola, S.B., Angelsen, A., Bruce, J.W., Xu, J., 2001. The causes of land-use and land-cover change: moving beyond the myths. *Global Environmental Change*, 11(4), pp.261-269. https://doi.org/10.1016/S0959-3780(01)00007-3.

Liu, Y., Song, W. and Deng, X., 2019. Understanding the spatiotemporal variation of urban land expansion in oasis cities by integrating remote sensing and multi-dimensional DPSIR-based indicators. *Ecological Indicators*, 96, pp.23-37. http://dx.doi.org/10.1016/j.ecolind.2018.01.029.

Lu, Y., Wu, P., Ma, X. and Li, X., 2019. Detection and prediction of land use/land cover change using spatiotemporal data fusion and the Cellular Automata–Markov model. *Environmental Monitoring and Assessment*, 191, pp.1-19. https://link.springer.com/article/10.1007%2Fs10661-019-7200-2.

Maktav, D. and Erbek, F.S., 2005. Analysis of urban growth using multi-temporal satellite data in Istanbul, Turkey. *International Journal of Remote Sensing*, 26(4), pp.797-810. http://dx.doi.org/10.1080/01431160512331316784.

Marcotullio, P.J. and Lee, Y.S.F., 2003. Urban environmental transitions and urban transportation systems: A comparison of the North American and Asian experiences. *International Development Planning Review*, 25(4), pp.325-354. http://dx.doi.org/10.3828/idpr.25.4.2.

Mas, J.F., Lemoine-Rodríguez, R., González-López, R., López-Sánchez, J., Piña-Garduño, A. and Herrera-Flores, E., 2017. Land use/land cover change detection combining automatic processing and visual interpretation. *European Journal of Remote Sensing*, 50(1), pp.626-635.

Masila, S.M., 2016. Effects of land degradation on agricultural land use: a case study of smallholder farmers indigenous knowledge on land use planning and management in Kalama division, Machakos county (Doctoral dissertation). http://dx.doi.org/10.9734/cjast/2019/v34i330134.

Mathews, A.J. and Nghiem, S.V., 2021. Examining Urban Built-up Volume: Three-Dimensional Analyses with Lidar and Radar Data. In: *Urban Remote Sensing: Monitoring, Synthesis, and Modeling in the Urban Environment*, pp.17-45. https://doi.org/10.1002/9781119625865.ch2.

Mohamed, A. and Worku, H., 2019. Quantification of the land use/land cover dynamics and the degree of urban growth goodness for sustainable urban land use planning in Addis Ababa and the surrounding Oromia special zone. *Journal of Urban Management*, 8(1), pp.145-158. https://doi.org/10.1016/j.jum.2018.11.002.

Mohan, R. and Dasgupta, S., 2004, June. Urban development in India in the twenty first century: policies for accelerating urban growth. In: *Fifth Annual Conference on Indian Economic Policy Reform*, Stanford Centre for International Development. Retrieved from http://scid.stanford.edu/sites/default/files/publications/231wp.pdf.

Montgomery, M.R., Stren, R., Cohen, B. and Reed, H.E., 2013. *Cities transformed: demographic change and its implications in the developing world*. Routledge. http://dx.doi.org/10.4324/9781315065700.

Munsi, M., Malaviya, S., Oinam, G. and Joshi, P.K., 2010. A landscape approach for quantifying land-use and land-cover change (1976–2006) in middle Himalaya. *Regional Environmental Change*, 10, pp.145-155. http://dx.doi.org/10.1007/s10113-009-0101-0.

Naikoo, M.W., Rihan, M. and Ishtiaque, M., 2020. Analyses of land use land cover (LULC) change and built-up expansion in the suburb of a metropolitan city: Spatio-temporal analysis of Delhi NCR using landsat datasets. *Journal of Urban Management*, 9(3), pp.347-359. https://doi.org/10.1016/j.jum.2020.05.004.

Ning, Y., Liu, S., Zhao, S., Liu, M., Gao, H. and Gong, P., 2022. Urban growth rates, trajectories, and multi-dimensional disparities in China. *Cities*, 126, p.103717. https://doi.org/10.1016/j.cities.2022.103717.

Nkeki, F.N., 2016. Spatio-temporal analysis of land use transition and urban growth characterization in Benin metropolitan region, Nigeria. *Remote Sensing Applications: Society and Environment*, 4, pp.119-137. http://dx.doi.org/10.1016/j.rsase.2016.08.002.

Padhi, B. and Mishra, U.S., 2022. Assessment of living condition of urban slum dwellers in India in the New Millennium. *Urban Research & Practice*, 15(4), pp.604-626.

Rauws, W.S. and de Roo, G., 2011. Exploring transitions in the peri-urban area. *Planning Theory & Practice*, 12(2), pp.269-284. http://dx.doi.org/10.1080/14649357.2011.581025.

Turner, B., Meyer, W.B. and Skole, D.L., 1994. Global land-use/land-cover change: towards an integrated study. *Ambio*, 23(1), pp.91-95. Available at: http://www.jstor.org/stable/4314168?origin=JSTOR-pdf.

Xie, Y., Mei, Y., Guangjin, T. and Xuerong, X., 2005. Socio-economic driving forces of arable land conversion: A case study of Wuxian City, China. *Global Environmental Change*, 15(3), pp.238-252. http://dx.doi.org/10.1016/j.gloenvcha.2005.03.002.

Yakub, M. and Tiffin, P., 2017. Living in the city: urban environments shape the evolution of a native annual plant. *Global Change Biology*, 23(5), pp.2082-2089. https://doi.org/10.1111/gcb.13528.

Yang, L., Xian, G., Klaver, J.M. and Deal, B., 2003. Urban land-cover change detection through sub-pixel imperviousness mapping using remotely sensed data. *Photogrammetric Engineering & Remote Sensing*, 69(9), pp.1003-1010. https://doi.org/10.14358/PERS.69.9.1003.

Yin, P., Li, X., Mao, J., Johnson, B.A., Wang, B. and Huang, J., 2023. A comprehensive analysis of the crop effect on the urban-rural differences in land surface phenology. *Science of The Total Environment*, 861, p.160604. https://doi.org/10.1016/j.scitotenv.2022.160604.

Younes, A., Ahmad, A., Hanjagi, A.D. and Nair, A.M., 2023. Understanding Dynamics of Land Use & Land Cover Change Using GIS & Change Detection Techniques in Tartous, Syria. *European Journal of Geography*, 14(3), pp.20-41. https://doi.org/10.48088/ejg.a.you.14.3.020.041.

Zhang, B., Li, W. and Zhang, C., 2022. Analyzing land use and land cover change patterns and population dynamics of fast-growing US cities: Evidence from Collin County, Texas. *Remote Sensing Applications: Society and Environment*, 27, p.100804. https://doi.org/10.1016/j.rsase.2022.100804.

Zhong, Y., Lin, A., He, L., Zhou, Z. and Yuan, M., 2020. Spatiotemporal dynamics and driving forces of urban land-use expansion: A case study of the Yangtze River economic belt, China. *Remote Sensing*, 12(2), p.287. https://doi.org/10.3390/rs12020287.

ORCID DETAILS OF THE AUTHORS

Govindaraju: https://orcid.org/0000-0002-0119-4826